Recent Progress in the Understanding of H Transport and Trapping in W

K. Schmid[1]‡, J. Bauer[1], T. Schwarz-Selinger[1], S. Markelj[2], U. v. Toussaint[1], A. Manhard[1], W. Jacob[1]

[1]Max-Planck-Institut für Plasmaphysik *Boltzmannstraße 2, D-85748 Garching b. München Germany*

[2]Jozef Stefan Institute *Jamova cesta 39, 1000 Ljubljana, Slovenia*

Abstract.

The retention of hydrogen isotopes (H, D and T) in the first, plasma exposed wall is one of the key concerns for the operation of future long pulse fusion devices. It affects the particle-, momentum- and energy balance in the scrape off layer as well as the retention of hydrogen isotopes (HIs) and their permeation into the coolant. The currently accepted picture that is used for interpreting current laboratory and tokamak experiments is that of diffusion hindered by trapping at lattice **defects**. This paper summarises recent results that show that this current picture of how HIs are transported and retained in W needs to be extended: The modification of the surface (e.g. blistering) can lead to the formation of fast loss channels for near surface HIs. Trapping at single occupancy traps with fixed de-trapping energy fails to explain isotope exchange experiments, instead a trapping model with multi occupancy traps and fill level dependent de-trapping energies is required. **The presence of interstitial impurities like N or C may affect the transport of solute HI**. The presence of HIs during damage creation by e.g. neutrons stabilises defects and reduces defect annealing at elevated temperatures.

1. Introduction

Transport of hydrogen isotopes (HI) in tungsten (W) first wall components affects many key processes in the operation of a fusion device: The balance between implantation into- and effusion out of the wall determines the recycling fluxes at the wall and thus affects the particle-, momentum- and energy balance in the scrape off layer (SOL). The transport of the implanted HIs into the bulk and its trapping at lattice defects determines the amount δ_{Ret} of retained tritium (T) in the wall, a value to be kept as low as possible to reduce the radioactive inventory and to conserve T as a precious resource. The permeation flux of T through the first wall material into the coolant

‡ Corresponding Author
Tel: +49 89 3299 2228
Fax: +49 89 3299 2279
E-mail: Klaus.Schmid@ipp.mpg.de

results in the formation of tritiated water which, due to its acidity, is difficult to handle and requires complex treatment to re-extract the T fuel from it. The currently applied model to interpret experimental data and to make predictions for future machines is that of diffusion of solute hydrogen being hindered by trapping/de-trapping at lattice defects. In this model description H exists in W in two populations: Solute at interstitial sites and trapped at lattice imperfections with high de-trapping energies. High thereby refers to the fact that at ambient temperatures the HIs cannot escape the trap sites. Solute H is transported by gradient-driven diffusion which is hampered by trapping. The traps immobilise the HIs until they de-trap and continue to diffuse. This exchange between solute and trapped state is described by the time evolution ($\frac{\partial C^T}{\partial t}$) of the trapped concentration of HIs (C^T). Therefore the dominating parameters affecting HI transport and retention are the density of lattice defects (η), their modification during plasma operation ($\eta \equiv \eta(x,t)$) and the way solute and trapped populations exchange ($\frac{\partial C^T}{\partial t}$).
The transport of H in W starts by H entering the W surface either by implantation or by gas phase uptake. A fraction Γ_{Surf} of this near surface solute H diffuses out of the surface and a fraction Γ_{Bulk} diffuses deeper into the bulk. Together they balance the incident flux $\Gamma_{In} = \Gamma_{Surf} + \Gamma_{Bulk}$. The ratio of Γ_{Bulk} / Γ_{Surf} is $<<$ 1 due to the shallow gradient into the bulk. Once the diffusing H reaches the back side, Γ_{Bulk} becomes the permeation flux Γ_{Perm}. Γ_{Bulk} is also an important contributor to the bulk retention, since it limits the rate at which bulk defects are decorated by HI that are then retained in the W-bulk. In current laboratory experiments typically only the HI retention & transport in the first few μm is experimentally accessible and therefore the interpretation of the results is strongly affected by the near surface evolution of η. In future fusion devices, due to high flux and temperature, the transport into the bulk and trapping at bulk defects will dominate. Therefore unless these near surface defects can modify Γ_{Bulk} **(e.g. by introducing an additional HI loss term in the above flux balance or affect the solute transport)** they will only play a minor role.
This paper will summarise recent results on the underlying processes affecting Γ_{Surf}, Γ_{Bulk}, η, $\frac{\partial C^T}{\partial t}$ and the resulting evolution of Γ_{Bulk} and δ_{Ret} under the conditions at the first wall of a fusion device: The modification of the surface (e.g. blistering or connected porosity from He implantation) can lead to the formation of fast loss channels for near surface H leading to a strong effective increase of Γ_{Surf} and a corresponding decrease in Γ_{Bulk} reducing both Γ_{Perm} and δ_{Ret}. Γ_{Bulk} is linked to Γ_{Surf} via the flux balance and depends on the solute diffusion coefficient D_{Sol} and η. D_{Sol} **is modified by the presence of nitride of carbide layers which feature a different** D_{Sol} **and thus** Γ_{Perm} **and** δ_{Ret}. Isotope exchange experiments have shown that the trapping process of H in W cannot be explained by the classic diffusion trapping picture of fixed de-trapping energies alone, but can be explained by a $\frac{\partial C^T}{\partial t}$ model of multi occupancy traps with fill level dependent de-trapping energies. The presence of HIs during damage creation by e.g. neutrons stabilises the created defects and reduces defect annealing at elevated temperatures.
The paper will first give an overview of the current picture of HI transport and trapping

in W followed by a comparison to the new concept of fill level dependent trapping required to understand isotope exchange at low temperatures. Then the mechanisms for defect production by the incident particle flux are discussed and the influence of surface modifications on the loss of HI from the surface are shown. Finally recent results on the influence of impurities are presented.

2. The diffusion trapping picture

The diffusion trapping picture has been very successful in explaining HI retention in W **both** qualitatively and in some cases quantitatively for typical experiments involving implantation (loading) of W by HIs and subsequent depth profiling by nuclear reaction analysis (NRA) and degassing by thermal effusion spectroscopy (TES) e.g. [1, 2].
Diffusion trapping codes [1, 3, 4] model the transport and trapping of HIs in W by distinguishing two HI populations: Interstitial solute HIs that can migrate through the material via diffusion and immobile, trapped HI bound in a particular trap. The exchange between the two populations (via trapping & de-trapping) is governed by processes with an Arrhenius type temperature dependence. The solute transport is simulated by applying Fick's second law of diffusion coupled to differential equations describing the exchange $\frac{\partial C^T}{\partial t}$ between solute and trapped HIs. The main equation for the diffusive transport and exchange with the trapped population is given in eq. 1

$$\frac{\partial C^{SOL}(x,t)}{\partial t} = D^{SOL}(T)\,\frac{\partial^2 C^{SOL}(x,t)}{\partial^2 x} + S(x,t) - \sum_{i=0}^{N^{Trap}-1}\frac{\partial C_i^T(x,t)}{\partial t} \qquad (1)$$

$C^{SOL}(x,t)$ = Concentration of solute hydrogen

$D^{SOL}(T)$ $= D_0\, exp\,(-E_D/k_BT)$
= Solute diffusion coefficient as function of temperature

$S(x,t)$ = Hydrogen source due to implantation with flux Γ $(m^{-2}s^{-1})$

The time evolution of the trapped population is described by eq. 2.

$$\frac{\partial C_i^T(x,t)}{\partial t} = \alpha_i(T)\,C^{SOL}(x,t)\left(\eta_i(x,t) - C_i^T(x,t)\right) - C_i^T(x,t)\,\beta_i(T) \qquad (2)$$

$C_i^T(x,t)$ = Concentration of hydrogen in trap type i

$\eta_i(x,t)$ = Concentration of trap type i

$\alpha_i(T)$ $= \nu_i^{ST}\exp\left(\frac{-E_i^{ST}}{K_BT}\right)$
= Arrhenius factor for trapping into trap i (s^{-1})

$\beta_i(T)$ $= \nu_i^{TS}\exp\left(\frac{-E_i^{TS}}{K_BT}\right)$
= Arrhenius factor for de-trapping from trap i (s^{-1})

An excellent derivation of these fundamental equations can be found in [5]. The main input parameter in eq. 1 is the solute diffusion coefficient. The commonly

accepted value for $D^{SOL}(T)$ is based on the experiments by Frauenfelder [6] which give an activation energy of $E_D = 0.39\ (eV)$ and pre-factor $4.1 \times 10^{-7}\ (m^2/s)$. Recent DFT based modelling [7] suggest a lower value of $E_D = 0.26\ (eV)$ which can also be extracted from Frauenfelders data by neglecting his $D^{SOL}(T)$ data at lower (< 2000 K).
Eq. 2 requires the Arrhenius parameters $\nu_i^{TS,ST}(s^{-1})$ and $E_i^{TS,ST}\ (eV)$ for each trap type i. The superscripts ST and TS thereby stand for "Solute to Trap for $\alpha_i(T)$" and "Trap to Solute for $\beta_i(T)$" respectively. Often, to reduce the number of free parameters, ν_i^{ST} and E_i^{ST} are approximated as $\nu_i^{ST} = D_0/a_0^2$ and $E_i^{ST} = E_D$ which amounts to assuming a diffusive step of one lattice constant a_0 is required to enter the trap.
In order to solve the coupled equations boundary conditions are required at the surface describing the effusion of HI from the material and if applicable the gas phase uptake. The commonly accepted picture for the surface processes on W is that of recombinative desorption by a Langmuir Hinslewood process for effusion from the surface and dissociative adsorption followed by a kinetically hindered uptake into the bulk [8]. However for typical laboratory implantation conditions, most experiments can be modelled with a much simpler boundary condition by assuming that effusion from the surface is limited by diffusion to the surface resulting in a simple Dirichlet boundary condition $C^{SOL} = 0$ at the surfaces. Also due to the high activation energy (heat of solution for H in W ≈ 1 eV [6]) for uptake into the bulk from a chemisorbed surface state, gas phase uptake can be neglected in cases where a volume HI source $S(x,t)$ by ion implantation is present.
By assuming equilibrium in eq. 2, $\frac{\partial C_i^T(x,t)}{\partial t} \equiv 0$ [5] the system of coupled equations can be rewritten as a single equation with an effective diffusion coefficient as shown in eq. 3 (see [5] for details of this variable transformation) The dependencies on x and t were omitted for brevity in eq. 3.

$$\begin{aligned}
\frac{\partial C^{SOL}}{\partial t} &= \frac{D^{SOL}(T)}{1+\Omega(T)}\frac{\partial^2 C^{SOL}}{\partial^2 x} + \frac{S}{1+\Omega(T)} \\
D_{Eff} &= \frac{D^{SOL}(T)}{1+\Omega(T)} \\
\Omega(T) &= \sum_{i=0}^{N^{Trap}-1} \frac{\partial C_i^T}{\partial C^{SOL}} \\
&= \sum_{i=0}^{N^{Trap}-1} \frac{\alpha_i(T)\left(\eta_i(x,t) - C_i^T\right)}{\beta_i(T)}
\end{aligned} \tag{3}$$

Equation 3 allows to estimate the regime where the diffusive transport is affected or even dominated by trapping i.e. where $\Omega(T) >> 1$. In Fig. 1 the ratio of the effective diffusion coefficient to the solute diffusion coefficient based on eq. 3 for typical trapping parameters in W is shown as function of temperature and solute concentration. The plot assumes a single trap with $\eta = 10^{-4}\ (at.frac.)$ $\nu^{TS} = 10^{13}\ s^{-1}$ and $E^{TS} = 1.4\ eV$. For α_i the above explained approximation via the solute diffusion coefficient is used.

From Fig. 1 three different regimes can be extracted: At high temperatures where β_i dominates over α_i all traps are essentially empty and $D_{Eff} \approx D^{SOL}$ only depends on temperature and not on solute concentration. At low temperature there is a strong dependence of HI transport on the solute concentration C^{SOL}. At a given temperature C^{SOL} mainly depends on the source strength $S(x,t)$. For low C^{SOL} all HIs that reach a certain depth are immediately immobilised (trapped) whereas for higher C^{SOL} the traps are saturated and any HIs that reach a depth, simply diffuse past the traps and are unaffected by them, since filled traps are assumed to be inactive. What Fig. 1 shows is that for most of the operating regime of a W first wall in a fusion device trapping will dominate HI transport. Therefore understanding the formation and evolution of traps is the key to predicting HI transport and retention in future fusion machines.

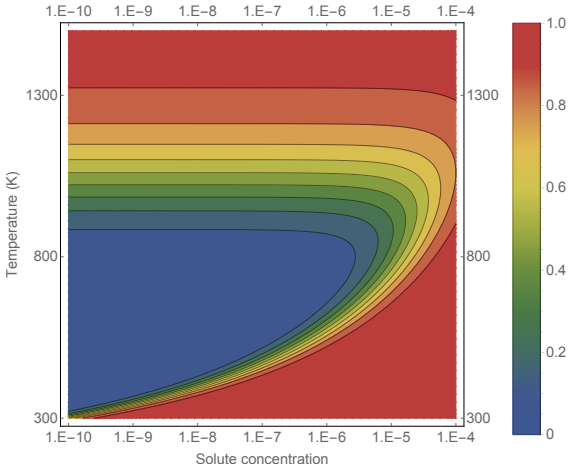

Figure 1. Ratio of the effective diffusion coefficient $\left(= \frac{1}{1+\Omega}\right)$ to the solute diffusion coefficient based on eq. 3 for typical trapping parameters in W (see text)

2.1. Fill level dependent trapping

In [9] the concept of multi-occupancy of traps was used to explain isotope exchange (see subsection 2.2) at low temperatures (R.T. to $\leq$ 450 K where $k_B * T << E^{TS}$). The idea is that every trap can store a certain number of HIs with a de-trapping energy that decreases with fill level up to the point where adding additional HIs is no longer energetically favourable. This idea is based on the results from DFT-calculations [10, 11] which predict that at low enough temperature up to 12 H-atoms can be trapped in a single mono-vacancy with de-trapping energies ranging from $\approx$ 1.4eV to 0.7eV.
For the details of the complex derivation of the fill level dependent trapping equations the reader is referred to [9]. Here only the final equations are summarised together with a basic explanation of their shape. In the fill level dependent picture the trapped concentration becomes $C^{ti}_{m,k}$: The concentration of an isotope of type m that is trapped in a trap of type ti with fill level k. The model treats the case of two isotopes $m \in \{A, B\}$. The fill level k means that the **sum** of atoms of type A plus the sum of atoms of type

B in the trap equals k. This results in a strong coupling between fill levels: Trapping into a trap at level k-1 moves all atoms to level k and accordingly increases $C^{ti}_{m,k}$ and decrease $C^{ti}_{m,k-1}$. Similarly de-trapping from level k moves all atoms to level k-1 and accordingly decreases $C^{ti}_{m,k}$ and increases $C^{ti}_{m,k-1}$. Since the actual amount of A and B at a particular level are not known (only their sum k is known) the amount of A and B that has to be moved between levels is described by the mean fractional occupancy $\Lambda^{ti}_{m,k}$ of level k with isotope m eq. 4.

$$\Lambda^{ti}_{m,k} = k\frac{C^{ti}_{m,k}}{C^{ti}_{A,k} + C^{ti}_{B,k}} \tag{4}$$

The amount of atoms of A and B that are trapped into or de-trap from level k are denoted by $\chi^{ti}_{m,k}(x,t)$ (s^{-1}) and $\psi^{ti}_{m,k}(x,t)$ (s^{-1}) respectively. It has to be kept in mind that trapping into k at a rate $\chi^{ti}_{m,k}(x,t)$ occurs at the expense of k-1 ($C^{ti}_{m,k-1}$ decreases) and benefits k ($C^{ti}_{m,k}$ increases) and that de-trapping from k at a rate of $\psi^{ti}_{m,k}(x,t)$ occurs at the expense of k ($C^{ti}_{m,k}\downarrow$) and increases k-1 ($C^{ti}_{m,k-1}\uparrow$). The de-trapping rate ψ is simple and equivalent to the classic model for each fill level. Based on Λ, χ and ψ the time evolution for the trapped amount can be written as in eq. 5. In eq. 5 the equations are given for A, the corresponding equations for B follow readily be exchanging A with B and B with A respectively.

$$\begin{aligned}
\frac{\partial C^{ti}_{A,k}}{\partial t} = {} & \left(\chi^{ti}_{A,k} + \chi^{ti}_{B,k}\right) \times \Lambda^{ti}_{A,k-1} + \chi^{ti}_{A,k} - \ (= \text{trapping into k}) \\
& \left(\chi^{ti}_{A,k+1} + \chi^{ti}_{B,k+1}\right) \times \Lambda^{ti}_{A,k} - \ (= \text{trapping into k+1}) \\
& \left(\psi^{ti}_{A,k} + \psi^{ti}_{B,k}\right) \times \Lambda^{ti}_{A,k} + \ (= \text{de-trapping from k}) \\
& \left(\psi^{ti}_{A,k+1} + \psi^{ti}_{B,k+1}\right) \times \Lambda^{ti}_{A,k+1} - \psi^{ti}_{A,k+1} \ (= \text{de-trapping from k+1}) \\
& \text{for } 1 < k < k^{ti}_{Max} \\
\frac{\partial C^{ti}_{A,k}}{\partial t} = {} & \left(\chi^{ti}_{A,k} + \chi^{ti}_{B,k}\right) \times \Lambda^{ti}_{A,k-1} + \chi^{ti}_{A,k} - \ (= \text{trapping into k}) \\
& \left(\psi^{ti}_{A,k} + \psi^{ti}_{B,k}\right) \times \Lambda^{ti}_{A,k} \ (= \text{de-trapping from k}) \\
& \text{for } k \equiv k^{ti}_{Max} \\
\frac{\partial C^{ti}_{A,1}}{\partial t} = {} & \chi^{ti}_{A,1} - \ (= \text{trapping into k} = 1) \\
& \left(\chi^{ti}_{A,2} + \chi^{ti}_{B,2}\right) \times \Lambda^{ti}_{A,1} - \ (= \text{trapping into k} + 1 = 2) \\
& \left(\psi^{ti}_{A,1} + \psi^{ti}_{B,1}\right) \times \Lambda^{ti}_{A,1} + \ (= \text{de-trapping from k} = 1) \\
& \left(\psi^{ti}_{A,2} + \psi^{ti}_{B,2}\right) \times \Lambda^{ti}_{A,2} - \psi^{ti}_{A,2} \ (= \text{de-trapping from k} + 1 = 2) \\
& \text{for } K \equiv 1
\end{aligned} \tag{5}$$

The cases $k \equiv k^{ti}_{Max}$ and $K \equiv 1$ are special because they only have one adjacent level so some contributions do not exist. For the details of Λ, χ and ψ the reader is referred to [9]. The coupling of eq. 5 to the solute transport equation happens analogous to the

classic diffusion trapping model with the notable difference of an additional sum over the different fill levels: $\left(\sum_{ti=1}^{N^{Traps}} \sum_{k=0}^{k_{Max}^{ti}} \frac{\partial C_k^{ti}(x,t)}{\partial t}\right)$. An important point is that despite their complexity and different structure the resulting HI transport and release for mono-isotopic experiments is essentially identical to what the classic diffusion trapping picture yields [9]. This is important, since the classic diffusion trapping models match a wide range of existing experimental data. An example of what these equations yield for isotope exchange is given in the next section.

2.2. Isotope exchange at low temperatures

Based on the classic trapping according to eq. 2, HIs are permanently immobilised at low temperatures $\beta_i(T_{Low}) \approx 0$. This means that if a trap site can only contain one HI-atom ($\equiv$ single occupancy) no exchange with the solute population is possible and any subsequently implanted HIs just diffuse past the trapped HIs. Therefore in the classic diffusion trapping picture isotope exchange is not possible at low temperatures. Recent experiments [12] however have shown that isotope exchange does take place even at low temperatures. To explain this discrepancy the concept of fill-level-dependent trapping was introduced in [9]. This allows to explain isotope exchange at low temperature as follows: Initially the W bulk is loaded with HI 'A' and once the source of A is turned off the highest fill-levels depopulate and leave the surface via out-diffusion of the solute until a fill level is reached that does not de-trap significantly at the current temperature. If the sample is subsequently loaded with HI 'B' the fill-levels are re-populated by 'B' and de-trapping can again occur from traps that are now filled with a mixture of HI 'A' and 'B'. Since all HI trapped in a trap filled to a particular level have the same de-trapping energy, this allows to exchange the previously trapped HI 'A' with 'B' from the solute i.e. isotope exchange occurs at low temperature by decreasig the de-trapping energy through repopulating the high fill-level of the traps by refilling them from the solute. Of course just exchanging the isotopes locally from trapped to solute is not permanent since the now solute isotope may be re-trapped while out-diffusing from the sample. Therefore the time to reach full isotope exchange also depends strongly on the de-mixing of the solute via a combination of re-trapping, de-trapping, out-diffusion and finally outgassing from the surface.

To show the effect of fill level dependent trapping on isotope exchange a set of D/H implantation in W experiments was modelled. The basic experimental concept is described in [12]. W samples (mirror polished + recrystallized 2000K) were damaged by 20 MeV W ions to 0.5 DPA. This is a difference to the experimental routine in [12] where samples with natural defect density were used. The advantage of self-damaging the samples is that the high defect concentrations are rather homogeneous in depth and allow for very accurate determination of depth profiles via NRA due to the good statistics of the spectra. The so prepared samples were loaded with D at a temperature T_{impl} (K) up to a fluence of Φ_D (m^{-2}). Then after a day at ambient temperature the samples were loaded with H again at T_{impl} up to a fluence of Φ_H (m^{-2}). The D and H

ion flux $\Gamma_{D,H}$ during loading was 5.5×10^{19} and 7.6×10^{19} $(m^{-2}s^{-1})$ respectively. The samples were loaded by plasma without biasing the sample resulting in mean D, H ion energies of $\approx 5\ eV$ due to the difference between plasma and floating potential. This gentle loading was used trying not to generate additional defects by the HI loading. The D loading and isotope exchange were investigated by thermal effusion spectroscopy (TES) and nuclear reaction analysis (NRA). From TES the temperature evolution of the D outgassing was determined restricting the model w.r.t. the fill level trapping parameters. From NRA the D depth profile was extracted which restricts the model w.r.t. the trap site concentration $\eta_i(x)$. In the experiments $T_{impl} = 450K$, Φ_D up to 1.5×10^{25} (m^2) and Φ_H up to 2.0×10^{25} (m^2) were used.
The code "TESSIM-X" that is used to model the experimental data implements both the classic diffusion trapping model and the fill level dependent one. To model the experiments diffusion limited boundary conditions were used $C^{SOL}(0,t) \equiv C^{SOL}(x_{Max},t) \equiv 0$. The implantation source $S(x,t)$ was approximated by a Gauss shaped implantation profile with center ($\approx$ 0.4 nm) and width ($\approx$ 1 nm) matching a range calculation by SDTrimSP [13, 14, 15]. The reflection coefficient $R_{D,H}$ of D and H was also taken from these SDTrimSP calculations and was used to scale to $\Gamma_{D,H}$ by $(1 - R_{D,H})$ to obtain the implanted fraction.
Based on the TES spectra and in order to limit the number of free parameters, only a single trap type with 3 fill levels was used to model the data. The trapping parameters are summarised in table 2.2.

# of HIs	ν_{TS} (s^{-1})	E^{TS} (eV)
1	10^{13}	1.7
2	10^{13}	1.38
3	10^{13}	0.8

Table 1. Trapping parameters used in the fill-level-dependent trapping model

The trap site concentration profile $\eta_1(x)$ was modelled after the NRA D-depth profiles and is shown together with the calculated depth profiles in Fig. 2. η_1 is dominated by the damage created by the 20 MeV W-ions which result in a homogeneous damage profile up to $\approx 2\mu m$. In the model the sample was loaded for 74h with D at a sample temperature of 450K which resulted in a maximum penetration depth of the diffusion front of $> 8\mu m$. During the 70 hours of isotope exchange (again at 450K) D was exchanged by H throughout the entire region decorated with D during the D-loading phase. Both the loading and the isotope exchange depth profile match the experimental data reasonably well. Also shown is a model prediction using the classic model which severely underestimates isotope exchange, especially near the surface.

In Fig. 3 the experimental TES obtained at 450K are compared to the modelled ones. These TES taken after D-loading prior to H isotope exchange match the calculated one both qualitatively and quantitatively suggesting that the parameters in Table 2.2

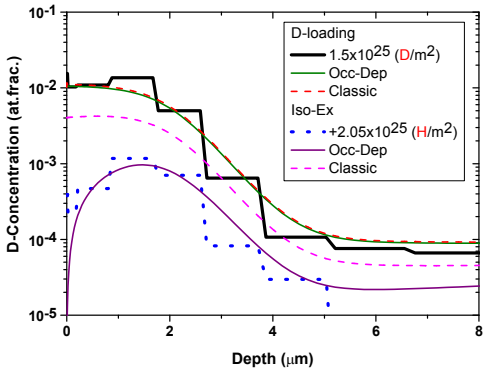

Figure 2. Comparison of experimental (stepped curves) and calculated D-depth profiles after D-loading and after subsequent isotope exchange with H. Both were performed at 450K

are reasonable. Also shown are the TES spectra as calculated by TESSIM-X using the classic, single occupancy diffusion trapping picture. For this calculation the three fill levels where converted into three distinct trap types each at a concentration $\frac{\eta_1(x)}{3}$ in order to match the total trap site concentration in both models. For the TES spectra after the pure D-loading there are only small differences between the two trapping models and they are qualitatively and quantitatively so similar that they cannot be distinguished within this mono-isotopic part of the experiment. However after isotope exchange the TES spectra of the remaining D in Fig. 3 are quite different in the two models: The occupancy dependent (Occ-Dep) model shows much stronger isotope exchange compared to the classic model. This results in a much higher retained D-amount after isotope exchange for the classic model compared the occupancy dependent model.

In Fig. 4 the evolution of the total amount of D retained in the samples is plotted

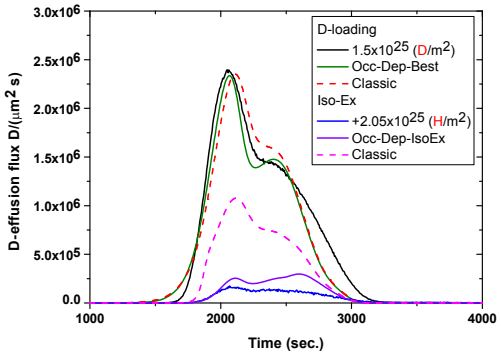

Figure 3. Comparison of experimental and calculated TES spectra at 450K before and after isotope exchange

as determined experimentally from NRA depth profiling. The Occ-Dep model matches

both the uptake speed during D-loading and the decay of the D-amount during isotope exchange with H. Similar as for the TES data the classic model is indiscernible from Occ-Dep model during the D-loading phase but fails to reproduce the depletion of the sample from D during the isotope exchange phase.
The discrepancy between the model and the data for the D-loading phase can be attributed to HI reflection coefficient at such low energies for which there only exist calculated data. In the simulation result presented here the reflection coefficient was taken SDTrimSP calculations and is in the order of 90%.

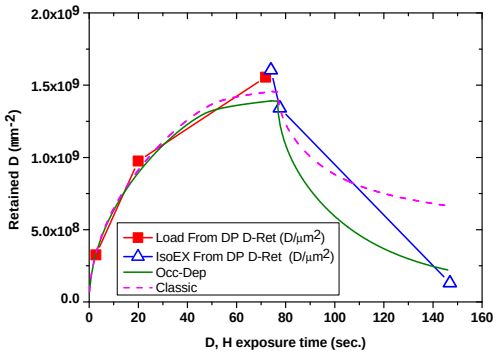

Figure 4. Comparison of experimental and calculated total retained amount of D after D-loading and after isotope exchange with H at 450K.

The occupancy dependent trapping model is required to understand isotope exchange at low temperatures. Isotope exchange mainly affects δ_{Ret} when switching the plasma operation from one HI species to another or during T removal prior to machine maintenance shutdown. Low temperature thereby always has to be considered as $k_B * T << E^{TS}$. Which means that for deep traps like the ones generated by n-damage for instance (see next section) low temperature can be significantly higher than ambient temperature.

2.3. Trap site production

As described in section 2 the retention and transport of HIs in W is dominated by traps over a wide range of first wall operating conditions. For predicting HI transport and retention in future fusion devices the knowledge of $\eta_i(x,t)$ is a key input and requires the understanding of defect formation and evolution. There are two main sources of trap site production in the first wall of a fusion experiment/reactor: Kinetic damage by fast particles, mainly by fast neutrons and defect production by the high solute HI concentration.
The damage cascades triggered by the primary knock-on W atoms hit by fast neutrons result in heavy damage throughout **centimetres** of W material [16]. In current experiments the defect production by n-irradiation in future fusion devices can only

be approximated: Todays fission reactors have a different n-energy distribution and the handling of highly activated W materials make retention measurements challenging. Therefore W-self-implantation by MeV W-ions was established as a **reasonable proxy for displacement damage during** n-irradiation [17]. Most of the experimental data on n-damage in W is based on self-implantation. There also exists data on real n-damaged materials [18] and the observed trends are comparable: Loading the damaged W material with D and investigating the inventory by NRA and TES shows that new deep ($E^{TS} \approx 1.8$ to 2.0 (eV)) traps are formed which result in TES release peaks at 800 to 1000K. At 300K the trap generation saturates at levels of $\eta \approx 10^{-2}$ (at.frac.)[19] which is much higher than intrinsic trap concentration levels in W which are of the order of 10^{-4} (at.frac) [20]. In self-damage experiments [21] the saturation of η is found at 0.2 to 0.5 displacements per atom (dpa) (as calculated by SRIM [22] with an assumed displacement energy of 90eV [23]). At elevated temperatures or after annealing the concentration of defects decreases [24, 19]. As shown in [24] and [25] the dominating defect in self-damaged W are dislocations and vacancy clusters.

The above cited experiments all performed damaging and D-loading sequentially therefore in order to investigate the potential interaction between retained D and defect generation, simultaneous loading and damaging experiments were performed in [26]. In these experiments W samples were damaged by MeV W-ions and simultaneously exposed to a D-atom beam at temperatures T_{exp} ranging from 600K to 1000K ($\equiv$ Simult.-damaging-loading). This simultaneous loading was compared to samples damaged at 300K with subsequent annealing to T_{exp} and D-loading at 600K ($\equiv$ Post-damage-annealing) and to samples damaged at T_{exp} and D-loading at 600K ($\equiv$ High-temp.-damaging). Comparing "Post-damage-annealing" with "High-temp.-damaging" showed a factor two decrease in the maximum D-concentration C^D_{MAX} in the NRA depth profile. This suggests that annealing of defects during damaging is more effective than post damaging annealing. For the "Simult.-damaging-loading" case, D-loading was performed at T_{exp} which is $\geq$ to the 600K D-loading temperatures in the other two cases. This higher temperature results in strong thermal de-trapping which would make it hard to compare to the other two cases. Therefore after the simultaneous damaging and loading the sample was loaded with D at 600 as in the other two cases to decorate the produced defects in a manner that makes the resulting C^D_{MAX} and total retention comparable to the other two cases. The results showed that the C^D_{MAX} from the "Simult.-damaging-loading" was in between the other two cases, so less defects were annealed compared to "High-temp.-damaging". This is a remarkable result since, due to the high temperatures, the amount of D present in W during damaging is extremely low and still this small **amount** of D during damaging stabilises the defects and partially prevents defect annealing.

One of the main differences between n-damage and damage by self-implantation is the damage production rate (dpa/sec). The expected dpa rate by n-irradiation in DEMO is $\approx 10^{-6}$ (dpa/s) [16] whereas for self-implantation the dpa rate is $\approx 10^{-4}$ (dpa/s). Therefore one could expect a difference in the produced number of defects. This was

investigated in [27] where a W sample was damaged by self-implantation at different damage rates, ranging from 10^{-5} to 10^{-2} (dpa/s) at temperatures of 290K and 800K. Then the sample was loaded with D at 290K at low ion energy in order not to create new defects and then the retained amount within the $\approx 2\mu m$ damaged near surface zone was measured by NRA. The resulting depth profiles at both temperatures showed no dependence of the retained D amount on the dpa rate supporting self-implantation as a viable proxy for n-irradiation displacement damage.

Exposing W surfaces to high HI ion fluxes strongly modifies the surface defect structure even when the particle energy is below the damage threshold [28, 29]. While the detailed mechanisms are not fully understood it is generally accepted that the high solute HI concentration is the driving force. While this dynamic solute inventory can hardly be measured directly, it can be calculated by diffusion trapping codes or from a simple flux balance if equilibrium between solute and trapped HI is assumed [30, 31] e.g. for the temperature of $\approx$ 500 K and high fluxes $10^{23}m^{-2}s^{-1}$ in [28] the expected solute concentration is of the order of $C^{SOL} \approx 10^{-5}$ $(at.frac.)$. In order to obtain such a concentration by gas loading at the same temperature, Sieverts law with a heat of solution of $\approx$ 1eV [6] and using the ideal gas law a pressure of $10^{18}Pa$ would be required. Of course such pressures are beyond the applicability of the ideal gas law but this still shows that 10^{-5} (at. frac.) is a very high concentration which is able to sustain high pressures in pores or cavities resulting in high stress fields in the surrounding lattice. According to [32, 10] high solute concentrations reduce the vacancy formation energy resulting in a high number of vacancies near the surface. This process of "super abundant vacancies" also exists for other metals [33] and their migration and clustering can lead to the formation of extended defects like vacancy clusters or dislocations.

These defects can then act as the nucleation sites [34] for gas filled cavities in the W matrix that are pressurised by the surrounding solute HI until the chemical potential inside the cavity matches that in the surrounding solute or the cavity bursts, opening a channel to the surface. These growing gas filled cavities can become visible at the surface and are commonly referred to as blisters (see [35, 36] and references therein). The formation of traps at sub-threshold energies is limited to the very near surface layer O (μm) and therefore at first glance, in contrast to n-damage which affects cm of W amor, is of little consequence w.r.t. the storage capacity of the wall for HIs. But as will be discussed in the next section the rupturing of blisters can have a substantial impact on the HI permeation rate.

3. Influence of surface morphology on effusion

Under high flux HI ion implantation high solute HI concentrations are reached near to the implantation surface (see previous section). This leads to modifications of the W surface morphology with blistering being the most prominent observation. **The formation of blisters has been the subject of numerous publications (see [37, 38] and references therein)**. The formation of blisters has different effects on

the migration and retention of HI in W which are summarised in Fig. 5.

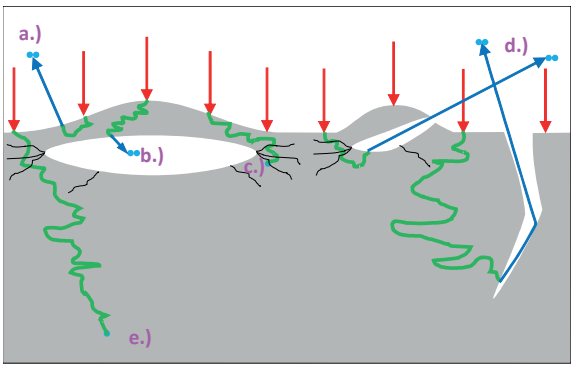

Figure 5. Influence of blisters and cracks on the transport and storage of HIs in W. a.) Degassing of implanted HI. b.) Trapping HIs as molecules in a closed blister. c.) Trapping of HIs in the dislocation network around a growing blister. d.) Loss of HI molecules from open cavities and cracks. e.) Trapping of HIs beyond the morphology affected area, deep in the bulk

Their formation results in a strong deformation of the near surface region resulting in a high concentration of dislocations [39] which act as trap sites for HI thus increasing δ_{Ret}. As long as the blister volume is closed it acts as a strong trap for HIs since the back reaction from the gas phase inside the blister to the surrounding W is kinetically hindered in particular at low temperatures and low HI pressures inside the blister due to the high endothermic heat of solution for HI in W [6]. Once the pressure inside the blister exceeds its stability limit the blister ruptures, releasing any stored HI gas. A ruptured blister also acts as a short cut from the blister cavity depth to surface for any HI diffusing into the blister: It can recombine at the blister cavity wall and degas from the surface as HI molecule. This can greatly enhance the loss of HI from the near surface regions as was shown in [31] and thus reduce the HI uptake into the W sample bulk and therefore also reduce permeation. In [31] part of the surface of W samples was first blistered by H ion implantation then the retained H was removed by heating the sample to 923 K in vacuum which does not lead to strong modification of the dislocation structure [20]. Then the entire sample was self-implanted with W ions to defect saturation, resulting in a homogeneous trap site distribution in- and outside of the blistered area. Finally the samples were loaded with D at 450K at a low energy of ≈ 5 eV per D to avoid further defect generation. Comparing the D uptake in the blistered and un-blistered area showed that the blistered area had a significantly reduced uptake of D and that the D depth profile in the blistered area had only reached a fraction of the depth as in the un-blistered area. This suggests that in blistered surfaces an additional loss channel exists for HI in the near surface region (i.e. blister depth) which most likely is outgassing via ruptured blister cavities. From flux conservation for a given Γ_{Surf} this loss channel must decrease Γ_{Bulk} and thus result in less permeation Γ_{Perm} through W. Similar to ruptured blister caps also cracks perpendicular to the plasma exposed W surface can result in enhanced degassing from the sample surface as qualitatively

depicted in Fig. 5.
Blisters are commonly associated with well polished samples used in laboratory experiments but recent studies [40] have shown that blisters also occur on rough and even technical surfaces. Thus this process of enhanced outgassing via ruptured blisters can also be significant for future fusion devices.

4. Influence of impurities on transport & trapping

The first wall in a fusion device is bombarded not only by the majority plasma HIs but also by a flux of impurity ions. These ions result from erosion of the first wall components (Be, C, W), are seeded into the SOL (Ar, N) to cool it or in the case of He, are intrinsic to the D+T fusion reaction.
As these impurity species are implanted into the surface as part of the plasma influx, they can potentially affect the transport of HI, by forming alloy (e.g. nitride or carbide) layers with different diffusion properties and/or increase δ_{Ret} by creating new near surface trap sites for HIs. While the creation of saturable trap sites is only a transient process that is negligible compared to bulk n-damage, affecting the diffusion properties can have a persistent effect on Γ_{Bulk} and thus Γ_{Perm}.
For N [41] and C [42] it was shown that the transport of HI through a N ($\approx 50\%N$) or C ($\approx 10\%C$) containing W layer is reduced. At these concentrations diffusion no longer takes place through W with impurities but through nitride or carbide containing regions. In particular for W+N in [41] essentially no transport of D through a WN layer was found at 300K whereas in pure W HI normally diffuse deep into the sample. Only at 600K diffusion of D through the WN layer became visible in the NRA depth profile.
For He the picture is more complex. According to [43, 44, 45] He pre- or co-implantation with HIs reduces the uptake and permeation of HIs for which two explanations are suggested in literature: Either the He containing surface layer that forms, reduces the solute diffusion coefficient, **similar to what has been shown for nitrides or carbides,** or He nano-bubbles form and result in connected porosity to the surface thus increasing out-gassing, similar to HI-induced blisters as described in section 3. In order to disentangle the two processes the He containing layer was moved into the bulk by high energy (MeV) He implantation in [46] . This allows to investigate a potential influence of He on HI diffusivity without being affected by a potential open porosity at the surface. In [46] W samples were damaged by self-implantation to trap density saturation and then the sample was loaded with D. Subsequently half of the sample was implanted with MeV He ions, resulting in a He containing layer well ($\approx 1\mu m$) below the surface **but still within the self-damaged region** ($\approx 2\mu m$). Due to the self-implantation to defect saturation the additional He should not introduce additional defects. Finally the sample was isochronally annealed and the propagation of D from the sample was investigated by NRA depth profiling. The experiment showed that in both halves of the sample, the D was diffusing out of the sample surface at the same rate suggesting that He does not

affect the solute diffusion coefficient. However the depth profiles showed that the He containing layer doubles the trap site density despite the already high trap level after self-implantation. This is probably due to an attractive interaction between He clusters in W and HIs. This experiment suggests that the hypothesis of reduced solute diffusion in the presence of He is less likely, leaving only the hypothesis of outgassing through connected porosity to explain the experimentally observed reduction in retention and permeation during He pre- and co-implantation.

5. Conclusions

The diffusion trapping picture of HI transport and retention in W is very successful at describing existing and predicting future fusion experiments. Recent experiments have shown that it needs to be extended to include new effects: To model low temperature isotope exchange the trapping picture has to be changed from single occupancy fixed de-trapping energy traps to multi-occupancy traps with fill level dependent de-trapping energies. A lot of experimental data is available on the formation of trap sites due to particle bombardment but no closed modelling solution exists that would allow to predict the trap density η_i as function of depth and time for a given set of exposure conditions (species, fluxes, energies and temperature) as required to include the trap density evolution in the diffusion trapping picture. Therefore introducing defect production and evolution is mostly included in an ad-hock fashion in modelling calculations. Similarly the influence of impurities on transport can be readily included in diffusion trapping models but most experiments only qualitatively show the effects the impurities have. **To properly include their influence quantitative numbers on the solute diffusion coefficient in alloy layers are needed**.
The influence of surface morphology on HI transport and retention is not straight forward to include in current diffusion trapping codes. This requires a 2D or even 3D treatment of the complex geometry spanning orders of magnitude from the implantation range to the blister depth / size and finally to the thickness of the W amor which is computationally challenging.

6. Acknowledgement

This work has been carried out within the framework of the EUROfusion Consortium and has received funding from the Euratom research and training programme 2014 - 2018 under grant agreement No 633053. The views and opinions expressed herein do not necessarily reflect those of the European Commission. The work was partially carried out under WP PFC.

[1] Schmid K, Rieger V and Manhard A 2012 *J. Nucl. Mat.* **426** 247
[2] Ogorodnikova O V, Roth J and Mayer M 2008 *J. Appl. Phys* **103** 34902
[3] Longhurst G R and Ambrosek J 2005 *Fusion Science and Technology* **48** 468
[4] Hodille E, Bonnin X, Bisson R, Angot T, Becquart C, Layet J and Grisolia C 2015 *J. Nucl. Mat.* **467** 424

[5] Krom A H M and Bakker A 2000 *METALLURGICAL AND MATERIALS TRANSACTIONS B* **31B** 1475
[6] Frauenfelder R 1969 *J. Vac. Sci. Technol.* **6(3)** 388
[7] Heinola K and Ahlgren T 2010 *J. Appl. Phys.* **107** 113531
[8] Pick M A and Sonnenberg K 1985 *J. Nucl. Mat.* **131** 208
[9] Schmid K, von Toussaint U and Schwarz-Selinger T 2014 *Journal of Applied Physics* **116** 134901
[10] Fernandez N, Ferro Y and Kato D 2015 *Acta Materialia* **94** 307
[11] Johnson D F and Carter E A 2010 *J. Mater. Res.* **25 No. 2** 315
[12] Roth J, Schwarz-Selinger T, Alimov V and Markina E 2013 *J. Nucl. Mat.* **432** 341
[13] Eckstein W, Dohmen R, Mutzke A and Schneider R 2007 *Report IPP, Garching* **12/3** URL http://hdl.handle.net/11858/00-001M-0000-0027-04E8-F
[14] Biersack J and Eckstein W 1984 *Appl. Phys. A* **34** 73
[15] Eckstein W 1991 *Computer Simulation of Ion-Solid Interactions* (Springer Verlag)
[16] Gilbert M, Dudarev S, Nguyen-Manh D, Zheng S, Packer L and Sublet J C 2013 *J. Nucl. Mat.* **442** 755
[17] Tyburska B, Alimov V, Ogorodnikova O, Schmid K and Ertl K 2009 *J. Nucl. Mat.* **395** 150
[18] Shimada M, Cao G, Otsuka T and et al 2015 *Nucl. Fusion* **55** 13008
[19] Markina E, Mayer M, Manhard A and Schwarz-Selinger T 2015 *J. Nucl. Mat.* **463** 329
[20] Manhard A, Schmid K, Balden M and Jacob W 2011 *J. Nucl. Mater.* **415** 632
[21] Alimov V, Hatano Y, Tyburska-Püschel B, Sugiyama K and et al 2013 *J. Nucl. Mat.* **441** 280
[22] Ziegler J F 2012 SRIM the stopping and range of ions in matter URL http://www.srim.org
[23] 2016 *E521 - 16: Standard Practice for Neutron Radiation Damage Simulation by Charged-Particle Irradiation* vol 12.02 (ASTM International Std.)
[24] Založnik A, Markelj S, Schwarz-Selinger T, Ciupinski L and et al 2016 *Physica Scripta* **T167** 014031
[25] Uytdenhouwen I, Schwarz-Selinger T, Coenen J W and Wirtz M 2016 *Phys. Scr.* **T167** 014007
[26] Markelj S, Schwarz-Selinger T, Založnik A, Kelemen M, Vavpetič P, Pelicon P, Hodille E and Grisolia C 2016 *Nuclear Materials and Energy* **In press** URL http://doi.org/10.1016/j.nme.2016.11.010
[27] Schwarz-Selinger T 2016 *Nuclear Materials and Energy* **In press** URL http://doi.org/10.1016/j.nme.2017.02.003
[28] Zayachuk Y and 't Hoen et al M 2013 *Nucl. Fusion* **53** 013013
[29] Gao L, Jacob W, von Toussaint U, Manhard A, Balden M, Schmid K and Schwarz-Selinger T 2017 *Nucl. Fusion* **57** 016026
[30] Schmid K 2016 *Phys. Scr.* **T167** 014025
[31] Bauer J, Schwarz-Selinger T, Schmid K, Balden M, Manhard A and von Toussaint U 2017 *Nuclear Fusion* **57** 086015
[32] Middleburgh S C, Voskoboinikov R E, Guenette M C and Riley D P 2014 *J. Nucl. Mat.* **448** 270
[33] Fukaia Y, Mizutani M, Yokota S and et al 2003 *J. Alloys and Comp.* **356-357** 270
[34] Terentyev D, Temmerman G D, Morgan T W, Zayachuk Y and et al 2015 *J. Appl. Phys.* **117** 083302
[35] Jia Y, Liu W, Xu B, Luo G N, Li C, Fu B and Temmerman G D 2015 *J. Nucl. Mater.* **463** 312
[36] Balden M, Manhard A and Elgeti S 2014 *J. Nucl. Mater.* **452** 248
[37] Federici G, Skinner C, Brooks J, Coad J and et al 2001 *Nuclear Fusion* **41** 1967
[38] Lindig S, Balden M, Alimov V K, Manhard A and et al 2011 *Physica Scripta* **T145** 014039
[39] Manhard A, von Toussaint U, Balden M, Elgeti S, Schwarz-Selinger T, Gao L, Kapser S and et al 2016 *Nuclear Materials and Energy* **In press**
[40] Manhard A, Balden M and von Toussaint U 2017 *Nuclear Fusion* **In Press** URL https://doi.org/10.1016/j.nme.2016.10.014
[41] Gao L, Jacob W, Meisl G, Schwarz-Selinger T, Höschen T, von Toussaint U and Dürbeck T 2016 *Nucl. Fusion* **56** 016004

[42] Tyburska B 2010 *Deuterium Retention in Carbon and Self-implanted Tungsten* vol IPP 17/24 (Garching: Max-Planck-Institut für Plasmaphysik) URL http://hdl.handle.net/11858/00-001M-0000-0026-F2F6-B
[43] Alimov V K, Tyburska-Püschel B and Hatano Y 2012 *J. Nucl. Mat.* **420** 370
[44] Lee H T, Tanaka H, Ohtsuka Y and Ueda Y 2011 *J. Nucl. Mat.* **415** 696
[45] Reinhart M, Kreter A, Buzi L and Rasinski M 2015 *J. Nucl. Mat.* **463** 1021
[46] Markelj S, Schwarz-Selinger T and Založnik A 2017 *Nuclear Fusion* **57** 064002